The Search for Homoaromatic Semibullvalenes. 6.[1] X-ray Structure and Charge Density Studies of 1,5-Dimethyl-2,4,6,8-semibullvalenetetracarboxylic Dianhydride in the Temperature Range 123−15 K

Richard Vaughan Williams* and Vijay R. Gadgil

Department of Chemistry, University of Idaho, Moscow, Idaho 83844-2343

Peter Luger,* Tibor Koritsanszky, and Manuela Weber

Institut für Kristallographie der Freien Universität Berlin, Takustrasse 6, D-14195 Berlin, Germany

Received August 21, 1998

The structure of the bisannelated semibullvalene **11**, which was originally predicted to be in a symmetrical homoaromatic ground state, was investigated by ultralow-temperature diffraction experiments down to 15 K and by related HF calculations. High-resolution X-ray data taken at 15 K ($\sin\theta/\lambda_{max} = 1.074$ Å^{-1}) provided a detailed electron density distribution that allowed a full topological analysis. The experimental and HF electron densities for **11** are in excellent accord. The electron density regions between C(2,8) clearly reveal a "normal cyclopropyl σ-bond" and very sparse density between C(4,6) corresponding with little or no interaction between these latter two centers. These results certainly confirm that in the solid state **11** is not homoaromatic. The experimental data at 15 K provide limiting values of structural parameters for a single tautomer of **11**. In particular, the C(2,8) and C(4,6) distances are extremely useful base values for a bisannelated semibullvalene with an exceptionally low activation barrier to the Cope rearrangement.

Introduction

The Cope rearrangement of semibullvalene (**1**) proceeds through the homoaromatic transition state **1c**[2] with an extremely small activation energy ($\Delta G^{\ddagger} \sim 6$ kcal/mol).[3,4] A major goal in semibullvalene research is to modify the semibullvalene nucleus in such a way as to result in a ground-state neutral homoaromatic molecule (the ground-state analogue of **1c**).[5−7] The most widely explored approach to this elusive goal stems from calculations by Dewar[8] and Hoffmann.[9] They independently predicted that substitution, as in **2**, with electron-withdrawing groups (A) at the 2, 4, 6, 8 and electron-donating groups (D) at the 1 and 5 positions of semibullvalene would lead to a reduction in the barrier to the Cope rearrangement or maybe even a homoaromatic ground state. Many Dewar−Hoffmann semibullvalenes have been prepared and studied, and while the activation energy for their Cope rearrangement is decreased compared with **1**, no example of a homoaromatic ground state molecule has been isolated.[7]

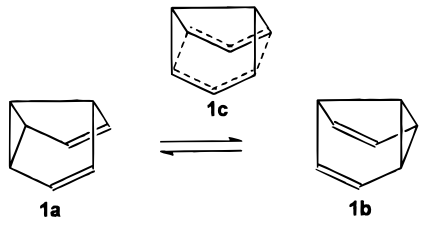

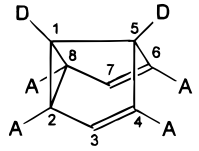

2

Another approach proposed to result in homoaromatic semibullvalenes is that of small-ring annelation. Paquette and Chamot suggested that in the bisannelated semibullvalene **3** the "breathing motion" of the Cope rearrangement may be inhibited, resulting, perhaps, in the favoring of the homoaromatic species.[10] Dannenberg et al., using the MNDO method, predicted that the 1,5-methano-annelated semibullvalene **4** would be homoaromatic.[11] Similarly, from AM1, MNDO, and PM3 (for the monoannelated **5** only) calculations, Williams and Kurtz suggested that the annelated semibullvalenes **5** and **6** should be homoaromatic.[1a−c] In a recent high-order

(1) (a) Part 1: Williams, R. V.; Kurtz, H. A. *J. Org. Chem.* **1988**, *53*, 3626. (b) Part 2: Williams, R. V.; Kurtz, H. A.; Farley, B. *Tetrahedron* **1988**, *44*, 7455. (c) Part 3: Williams, R. V.; Kurtz, H. A. *J. Chem. Soc., Perkin Trans. 2* **1994**, 147. (d) Part 4: Willams, R. V.; Gadgil, V. R.; Chauhan, K.; van der Helm, D.; Hossain, M. B.; Jackman, L. M.; Fernandes E. *J. Am. Chem. Soc.* **1996**, *118*, 4208. (e) Part 5: Willams, R. V.; Gadgil, V. R.; Chauhan, K.; Jackman, L. M.; Fernandes E. *J. Org. Chem.*, **1998**, *63*, 3302.

(2) (a) Jiao, H.; Nagelkerke, R.; Kurtz, H. A.; Williams, R. V.; Borden, W. T.; Schleyer, P. v. R. *J. Am. Chem. Soc.* **1997**, *119*, 5921. (b) Jiao, H.; Schleyer, P. v. R. *Angew. Chem., Int. Ed. Engl.* **1993**, *32*, 1760.

(3) Cheng, A. K.; Anet, F. A. L.; Mioduski, J.; Meinwald, J. *J. Am. Chem. Soc.* **1974**, *96*, 2887.

(4) Moskau, D.; Aydin, R.; Leber, W.; Günther, H.; Quast, H.; Martin, H.-D.; Hassenrück, K.; Miller, L. S.; Grohmann, K. *Chem. Ber.* **1989**, *122*, 925.

(5) See, for example, refs 1, 2, 6, and 7 and references therein.

(6) Williams, R. V.; Kurtz, H. A. *Adv. Phys. Org. Chem.* **1994**, *29*, 273.

(7) Williams, R. V. *Adv. Theor. Interesting Mol.* **1998**, *4*, 157.

(8) Dewar, M. J. S.; Lo, D. H. *J. Am. Chem. Soc.* **1971**, *93*, 7201.

(9) Hoffmann, R.; Stohrer, W.-D. *J. Am. Chem. Soc.* **1971**, *93*, 6941.

(10) Chamot, E.; Paquette, L. A. *J. Org. Chem.* **1978**, *43*, 4527.

(11) Miller, L. S.; Grohmann, K.; Dannenberg, J. J. *J. Am. Chem. Soc.* **1983**, *105*, 6862.

10.1021/jo981703q CCC: $18.00
Published on Web 01/30/1999

ab initio and DFT study of the semibullvalenes **1** and **4**−**8**, **1c** and **4**−**7** were judged to be homoaromatic using geometric, energetic, and magnetic criteria.[2a] These results are in complete accord with earlier semiempirical calculations[1a,c−e] and fully support the continued use of these economical methods for the prediction of homoaromaticity in semibullvalenes and related systems.

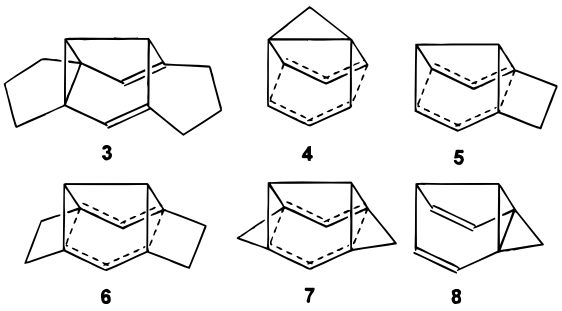

It is not a trivial matter to verify experimentally that a particular semibullvalene has a homoaromatic ground state.[6,7] On first consideration, single-crystal X-ray structure determination would appear to be the method of choice for appropriately crystalline samples. A homoaromatic semibullvalene should exhibit considerable symmetry with bond/interatomic distance equalization, while a localized (Cope) semibullvalene would be expected to be asymmetric. X-ray crystallography at ambient temperature on the β-form of the dinitrile **9** indicated a structure with apparent C_2 symmetry.[12] The usual conclusion from this observation would be that **9** is homoaromatic. However, variable-temperature solid-state ^{13}C CP-MAS NMR spectroscopy revealed that **9** is a Cope system undergoing rapid equilibration between nondegenerate tautomers.[12] At ambient temperature there is accidental degeneracy of the two tautomers, which results in the apparent C_2 symmetry observed in the X-ray structure at this temperature. These conclusions account for the confusing observations in the variable-temperature X-ray study of the isomeric dinitrile **10** in which the C(2,8) distance decreases and the C(4,6) distance increases with decreasing temperature.[13] Again in the solid state, **10** is a Cope system composed of equilibrating nondegenerate tautomers. As the temperature decreases, the population of the lower energy form increases and the C(2,8) and C(4,6) distances reflect this change. Quast proposes that this solid-state Cope rearrangement between nondegenerate tautomers is a general phenomenon and can be used to explain the anomalous X-ray data found for many semibullvalenes.[14] Quast also considers that the sum $\sum_r$ of the C(2,8) and C(4,6) distances is a molecular property and can be used in the characterization of the semibullvalenes.

Using the same semiempirical methods and discriminators[1b] as mentioned above, Williams et al. predicted that the bisanhydride **11** has a homoaromatic ground state.[1d,e] Supporting this conclusion, the variable-temperature solution-phase ^{13}C (125 MHz) and solid-state ^{13}C CP-MAS NMR spectra of **11** are temperature independent over the range 298−183 K and 293−223 K, respectively.[1d,e] Again

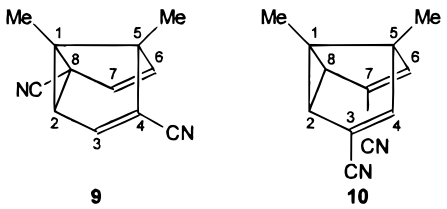

in support of a homoaromatic ground state, the single-crystal X-ray structures of **11** determined at 293, 243, and 163 K indicated apparent C_2 symmetry.[1d,e] However, at lower temperatures (148 and 123 K) X-ray structures indicate symmetry was broken and that Cope equilibration between nondegenerate tautomers was apparently occurring.[1d,e] NMR studies using a modification[15] of the Saunders' isotopic perturbation method[16] demonstrated that the anhydride **11** was also a localized Cope system in the solution phase.[1d,e] An estimate of the upper limit for the solution phase barrier to the Cope rearrangement ($\Delta G^{\ddagger}$ < 3.3 kcal/mol) was made from the variable-temperature ^{13}C NMR spectra of **11**.

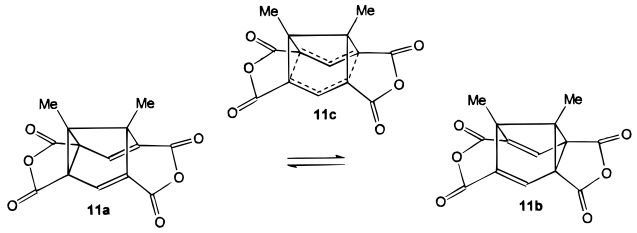

An unusual feature of **11** in the solid state, when compared with other previously studied semibullvalenes,[12−14,17] is its apparent C_2 symmetry over a *very wide* temperature range. This apparent symmetry likely results from equal population of **11a** and **11b**, and consequently, over this temperature range the equilibrium constant, *K*, for the solid-state Cope rearrangement of **11** must be unity. The unusual properties of **11** render it a most interesting candidate for further study in the solid state. Perhaps further insight into the solid-state Cope equilibrium and even the "frozen" C(2,8) and C(4,6) internuclear distances for a single tautomer of **11** are available from a X-ray crystallographic study over an extended temperature range. With the limiting values for the C(2,8) and C(4,6) distances in hand it would be possible to use Quast's method[14] to estimate the relative populations of the tautomeric states (**11a** and **11b**) for each temperature at which Cope equilibrium is taking place. Furthermore, the equilibrium constants obtained from the above data could be used to ascertain an approximate free energy difference between **11a** and **11b** in the solid state.

X-ray Experiments

Pale yellow prismatic crystals were grown from dry ethyl acetate/hexanes. A crystal with dimensions 0.58 × 0.41 × 0.23 mm was fixed with Araldite glue on a beryllium needle as described previously[18] and sealed in a capillary (0.01 mm wall thickness) to prevent sublimation of the crystal in the vacuum.

(12) Jackman, L. M.; Benesi, A.; Mayer, A.; Quast, H.; Peters, E.-M.; Peters, K.; von Schnering, H. G. *J. Am. Chem. Soc.* **1989**, *111*, 1512.
(13) Sellner, I.; Schuster, H.; Sichert, H.; Sauer, J.; Nöth, H. *Chem. Ber.* **1983**, *116*, 3751.
(14) Quast, H.; Carlsen, J.; Janiak, R.; Peters, E.-M.; Peters, K.; von Schnering, H. G. *Chem. Ber.* **1992**, *125*, 955.
(15) Gompper, R.; Schwarzensteiner, M.-L.; Wagner, H.-U. *Tetrahedron Lett.* **1985**, *26*, 611.
(16) Siehl, H.-U. *Adv. Phys. Org. Chem.* **1987**, *23*, 63.
(17) Macho, V.; Miller, R. D.; Yannoni, C. S. *J. Am. Chem. Soc.* **1983**, *105*, 3735.
(18) Zobel, D.; Luger, P. *J. Appl. Crystallogr.* **1990**, *23*, 175.

Table 1. X-ray Experimental Details for 11 in the Temperature Range 123−15 K

	TET123	TET80	TET40	TET15
temp (K)	123	80	40	15
chemical formula	$C_{14}H_8O_6$	$C_{14}H_8O_6$	$C_{14}H_8O_6$	$C_{14}H_8O_6$
chemical fw	272.20	272.20	272.20	272.20
cell setting	monoclinic	monoclinic	monoclinic	monoclinic
space group	*Cc*	*Cc*	*Cc*	*Cc*
a (Å)	10.326(2)	10.326(2)	10.317(1)	10.312(1)
b (Å)	11.456(2)	11.418(2)	11.389(2)	11.379(2)
c (Å)	10.139(2)	10.144(2)	10.142(1)	10.131(1)
β (deg)	111.80(1)	111.89(2)	111.92(1)	111.91(1)
V (Å^3)	1113.6(4)	1109.8(4)	1105.2(2)	1102.9(2)
Z	4	4	4	4
D_x (Mg m^{-3})	1.624	1.629	1.635	1.639
radiation type	Mo Kα	Mo Kα	Mo Kα	Mo Kα
wavelength	0.70932	0.70932	0.70932	0.70932
sin θ/λ_{max} (Å^{-1})	0.746	0.746	0.746	1.074
μ (mm^{-1})	0.130	0.130	0.131	0.131
abs corr	yes	yes	yes	yes
no. of measured reflns	1988	3946	3833	10721
no. of unobserved reflns ($F < 2\sigma$)	316	438	296	2276
R_{int}		2.0	2.3	3.8
refinement on	F^2	F^2	F^2	F^2
$R[F^2 > 4\sigma(F^2)]$	0.042	0.033	0.036	0.035
$wR(F^2)$	0.118	0.088	0.085	0.091
GoF	1.099	1.088	1.084	1.102

Figures of Merit for the Multipole Refinement

	m1	m2
NREF ($F_o > 3\sigma(F_o)$)	4072	4072
N_{var}	349	241
$R(F)$	0.028	0.030
$R_w(F)$	0.023	0.025
GoF	1.60	1.73
$R(F^2)$	0.038	0.041
$R_w(F^2)$	0.045	0.049

Since the crystals were slightly hygroscopic, preparation work was done under nitrogen atmosphere in a glovebox. The X-ray measurements were performed on a large Huber four-circle diffractometer (400 mm diameter, type 512) with offset χ circle, equipped with a double-stage closed cycle He refrigerator (Air products, Displex DE202) and a Be vacuum chamber around the cold head. The vacuum was achieved using a turbomolecular pump to reduce the pressure to less than 1×10^{-4} mbar (1 bar 10^5 Pa) and was stable during the entire measurement. After a rough data collection at room temperature, which was mainly executed to check the crystal quality and to confirm the previous structure results of Williams et al.,[1d] the crystal was cooled to 15 K with a cooling rate of 0. 1 deg min^{-1}. During the cooling procedure, which took about 2 days (attempts with shorter cooling periods led to mechanical destructions of the crystals), several reflections were inspected by ω-scans to monitor the crystal quality. The aligment of the crystal when hidden from view inside the Be chamber was controlled by the C8 routine[19] based on centering of one reflection in eight equivalent positions. During the cooling of the crystal from room temperature to 15 K, no discontinuous trend in lattice constants was observed. The temperature was measured with an Au(Fe)/chromel thermocouple fixed in a small hole at the tip of the second stage of the cryostat and was calibrated via a Si diode, fixed close to it. Temperature could be kept stable better than ±0.5° for weeks. For all X-ray experiments Nb-filtered Mo Kα radiation was used at 50 kV and 40 mA. At each of the temperatures listed in Table 1 intensity data were collected in the $\omega-2\theta$-scan mode including intensity profile recording. Except for the lowest temperature $2\theta_{max}$ was set to 64°. At 15 K high-order data were measured up to $2\theta = 100°$, to allow for a detailed electron density analysis. Three standard reflections were measured every 90 min, showing in no case a significant variation. In addition to the usual Lp-correction an analytical absorption correction (XTAL program system, version 3.2[20]) was applied. For further details of data collection see Table 1.

(19) King, H. E.; Finger, L. W. *J. Appl. Crystallogr.* **1979**, *12*, 374.

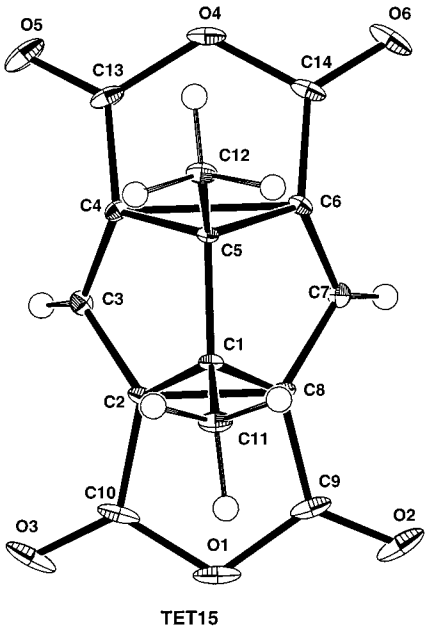

Figure 1. Molecular structure of **11** at 15 K in an ORTEP representation.[41] Thermal ellipsoids are plotted at a 50% probability scale.

Structure Refinement

From the 15 K data set a structure solution with direct methods (program SHELXS[21]) was obtained in the space group *Cc*. Since a significantly non C_2 symmetric molecular model was obtained (see Figure 1), which could not have a molecular 2-fold axis, the space group *C*2/*c*, being present for the room-temperature structure, was not further considered. Later the atomic positional and displacement parameters of a lower temperature data set were taken as input for the next higher temperature data. Conventional full-matrix least-squares refinements minimizing the quantity $\sum w(F_o^2 - kF_c^2)^2$ with $w = 1/[\sigma^2(F_o^2) + (ap)^2 + bP]$ (P ($F_o^2 + 2F_c^2$)/3 a, b optimized during the least-squares procedures) were executed using SHELXL.[22] Standard atomic parameters (anisotropic for C and O, isotropic for H) were used in the refinement that ran smoothly to convergence at all temperatures, yielding agreement factors listed in Table 1.

Multipole Refinement

The high-resolution (sin $\theta/\lambda \leq 1.074$ Å^{-1}) data set collected at 15 K was used to obtain accurate geometrical parameters and the charge density. The generalized scattering factor model based on the Hansen−Coppens formalism[23] was applied. The starting atomic parameters were taken from the conventional refinement. The refinements were carried out with the full-matrix LSQ program (XDLSM) of the XD program package.[24] In all cases the quantity $\sum_H w_H(|F_{obs}(H) - k|F_{cal}(H)|)^2$ was minimized using the statistical weight $w_H = \sigma^{-2}(F_{obs}(H))$ and only those structure factors that met the criteria of $F_{obs}(H) > 3\sigma(F_{obs}(H))$. The core and the spherical valence density were composed of Hartree−Fock wave functions expanded over

(20) Hall, S. R., Flack, H. D., Stewart, J. M., Eds. *XTAL Program System 3.2 User's Manual*; Universities of Western Australia, Geneva, and Maryland, 1992.

(21) Sheldrick, G. M.; Krüger, C.; Goddard, R. *Crystallographic Computing 3*; Oxford University Press: Oxford, 1985; pp 175−189.

(22) Sheldrick, G. M. *SHELXL-93, A Program for Refinement of Structures*; Universität Göttingen, 1995.

(23) Hansen, N. K.; Coppens, P. *Acta Crystallogr.* **1978**, *A34*, 909.

Table 2. Definition of the Local Atomic Coordinate System[c]

ATOM	ATOM 0	AX 1	ATOM 1	ATOM 2	AX 2	SITESYM	constrained to
O(1)	DUM0[a]	*z*	C(9)	C(10)	*x*	MM2	
O(2)	C(9)	*z*	O(2)	O(1)	*x*		
O(3)	C(10)	*z*	O(3)	O(1)	*x*		O(2)
O(4)	DUM1[b]	*z*	C(13)	C(14)	*x*	MM2	
O(5)	C(13)	*z*	O(5)	O(4)	*x*		
O(6)	C(14)	*z*	O(6)	O(4)	*x*		O(5)
C(1)	C(11)	*x*	C(1)	C(5)	*y*	M	
C(2)	C(8)	*z*	C(2)	C(1)	*y*		
C(3)	H(2)	*x*	C(3)	C(4)	*y*	M	
C(4)	C(6)	*z*	C(4)	C(5)	*y*		
C(5)	C(12)	*x*	C(5)	C(1)	*y*	M	
C(6)	C(4)	*z*	C(6)	C(5)	*y*		C(4)
C(7)	H(1)	*x*	C(7)	C(6)	*y*	M	C(3)
C(8)	C(2)	*z*	C(8)	C(1)	*y*		C(2)
C(9)	O(2)	*x*	C(9)	O(1)	*y*	M	
C(10)	O(3)	*x*	C(10)	O(1)	*y*	M	C(9)
C(11)	C(1)	*z*	C(11)	H(5)	*x*	3M	
C(12)	C(5)	*z*	C(12)	H(8)	*x*	3M	C(11)
C(13)	O(5)	*x*	C(13)	O(4)	*y*	M	
C(14)	O(6)	*x*	C(14)	O(4)	*y*	M	C(13)
H(1)	C(7)	*z*	C(7)	C(6)	*y*		
H(2)	C(3)	*z*	C(3)	C(4)	*y*		H(1)
H(3)	C(11)	*z*	C(11)	C(1)	*y*		
H(4)	C(11)	*z*	C(11)	C(1)	*y*		H(3)
H(5)	C(11)	*z*	C(11)	C(1)	*y*		H(3)
H(6)	C(12)	*z*	C(12)	C(5)	*y*		H(3)
H(7)	C(12)	*z*	C(12)	C(5)	*y*		H(3)
H(8)	C(12)	*z*	C(12)	C(5)	*y*		H(3)

[a] DUM0 1.08455 0.14977 1.29959. [b] DUM1 1.34677 0.12679 0.49971. [c] The AX1, AX2 plane is defined by the ATOM 0−ATOM and ATOM 2−ATOM 1 vectors. The third axis is taken perpendicular to this plane.

Slater-type basis functions.[25] For each heavy atom in different chemical environment a different radial screening parameter (κ) was assigned and refined. For the deformation terms single-ζ orbitals with energy-optimized Slater exponents were taken and kept fixed. The level of the expansion was hexadecapolar and dipolar for the heavy and for the hydrogen atoms, respectively. The atomic numbering used is shown in Figure 1, while the definition of the atomic site coordinate systems can be found in Table 2. Since the structure is noncentrosymmetric, the treatment of the data should be done with special care to avoid indeterminancies in the parameter estimates.[26] A feasible approach is to impose chemical symmetry on the density model in order to reduce the number of multipole populations to be refined. The isolated molecule is expected to possess a mirror symmetry which, though not present in the crystal structure, was invoked. The density associated with the two terminal O C−O−C O segments was also kept the same. Further local symmetry restrictions, detailed in Table 2, were applied to all atoms except for the carbonyl oxygens. The molecule was kept neutral during the refinement. To avoid the shortening of the C−H bond distances, their values were fixed at 1.08 Å. Several different isotropic extinction models[27] were tested with no indication for a need for correction. The parametrization outlined above and referred to as model m1 corresponds to a "conventional" multipole refinement in which a scale factor, the atomic positions (58), and anisotropic (120) and isotropic (8) temperature parameters of the heavy and of the hydrogen atoms, respectively, were refined together with their charge density parameters (163).

Table 3. Difference Mean-Square Displacement Amplitude for Bonds (Δ_{12}) [10^4 Å^2]

bond	model HF/6-311G**	model m1
O(1)−C(9)	2	−10
O(1)−C(10)	2	−1
O(4)−C(13)	3	8
O(4)−C(14)	3	7
O(2)−C(9)	0	−3
O(3)−C(10)	0	−1
O(5)−C(13)	1	7
O(6)−C(14)	1	7
C(8)−C(9)	3	5
C(2)−C(10)	3	−6
C(7)−C(8)	−3	−3
C(3)−C(2)	−3	0
C(6)−C(7)	−1	7
C(4)−C(3)	−1	0
C(14)−C(6)	−2	−6
C(13)−C(4)	−2	0
C(1)−C(11)	6	0
C(5)−C(12)	6	1
C(1)−C(2)	0	−7
C(1)−C(8)	0	−2
C(5)−C(4)	0	2
C(5)−C(6)	0	8
C(1)−C(5)	0	12
C(4)−C(6)	0	10
C(2)−C(8)	0	−4

Table 4. ΔMSDA for 1−3 Links (Δ_{13}) [10^4 Å^2]

1−3 link	model HF/6-311G**	model m1
C(10)−C(9)	0	−9
C(13)−C(14)	0	4
O(1)−O(2)	3	0
O(1)−O(3)	3	23
O(4)−O(5)	3	11
O(4)−O(6)	3	30
O(1)−C(8)	−1	−6
O(1)−C(2)	−1	−3
O(4)−C(4)	−1	3
O(4)−C(6)	−1	−7
O(2)−C(8)	−5	−3
O(3)−C(2)	−5	6
O(5)−C(4)	−5	0
O(6)−C(6)	−5	6
C(9)−C(7)	0	−3
C(10)−C(3)	0	4
C(9)−C(2)	4	8
C(10)−C(8)	4	4
C(8)−C(6)	1	−1
C(2)−C(4)	1	−1
C(7)−C(14)	0	−4
C(3)−C(13)	0	3
C(7)−C(4)	0	2
C(3)−C(6)	0	12
C(13)−C(6)	5	12
C(14)−C(4)	5	6
C(5)−C(11)	10	4
C(1)−C(12)	10	8
C(11)−C(8)	−6	−1
C(11)−C(2)	−6	−4
C(12)−C(4)	−8	−8
C(12)−C(6)	−8	−8

According to Hirshfeld's rigid-bond criterion[28] the bond projected components of the mean-square displacement (MSD) tensors for a bonded atom pair of comparable mass should not differ markedly. A departure from this postulate is a sign for bias in the ADPs (anisotropic displacement parameters) and,

(24) Koritsanszky, T.; Howard, S.; Richter, T.; Su, Z.; Mallinson, P. R.; Hansen, N. K. *XD: a Computer Program Package for Multipole Refinement and Analysis of Electron Densities from Diffraction Data. User Manual*; Free University Berlin, 1995.

(25) Clementi, E.; Roetti, C. *At. Data Nucl. Data Tables* **1974**, *14*, 177.

(26) El-Haouzi, A.; Hansen, N. K.; Lettrnaff, C.; Protas, J. *Acta Crystallogr.* **1996**, *A52*, 291.

(27) Becker, P. J.; Coppens, P. *Acta Crystallogr.* **1974**, *A30*, 129.

(28) Hirshfeld, F. L. *Acta Crystallogr.* **1976**, *A32*, 239.

Table 5. Selected Experimental and Optimized Bond Distances [Å]

bond	experimental 15 K convent. refinem.	average	experimental 15 K multipole	average	optimized form 11a HF/6-311G**
C(2)−C(8)	1.670(1)		1.6674(12)		1.602
C(2)−C(1)	1.504(1)	1.505(1)	1.5023(10)	1.5032(10)	1.495
C(8)−C(1)	1.506(1)		1.5041(10)		
C(1)−C(5)	1.544(1)		1.5429(7)		1.547
C(4)−C(5)	1.519(1)	1.519(1)	1.5193(10)	1.5194(10)	1.520
C(6)−C(5)	1.520(2)		1.5194(10)		
C(2)−C(10)	1.475(1)	1.475(1)	1.4734(10)	1.4741(10)	1.487
C(8)−C(9)	1.476(1)		1.4748(10)		
C(2)−C(3)	1.443(1)	1.443(1)	1.4421(10)	1.4442(11)	1.466
C(8)−C(7)	1.444(1)		1.4462(11)		
C(4)−C(13)	1.468(1)	1.468(1)	1.4678(10)	1.4681(11)	1.483
C(6)−C(14)	1.469(1)		1.4684(11)		
C(3)−C(4)	1.352(1)	1.352(1)	1.3555(12)	1.3545(12)	1.329
C(7)−C(6)	1.352(1)		1.3534(10)		
C(1)−C(11)	1.498(1)		1.4996(11)		1.510
C(5)−C(12)	1.511(1)		1.5094(10)		1.523
C(10)−O(1)	1.393(2)	1.390(2)	1.3916(13)	1.3905(13)	1.360
C(9)−O(1)	1.387(2)		1.3893(13)		
C(10)−O(3)	1.191(2)	1.191(2)	1.1959(14)	1.1946(14)	1.166
C(9)−O(2)	1.191(2)		1.1932(14)		
C(13)−O(4)	1.394(1)	1.393(2)	1.3897(11)	1.3931(12)	1.369
C(14)−O(4)	1.393(2)		1.3965(12)		
C(13)−O(5)	1.199(1)	1.198(1)	1.1975(12)	1.1950(12)	1.167
C(14)−O(6)	1.197(1)		1.1924(12)		
C(4)−C(6)	2.206(1)		2.2051(12)		2.237

consequently, in the multipole populations. Tables 3 and 4 compares the difference MSD amplitudes for bonds (Δ_{12}) and for the closest links (Δ_{13}) with those calculated from ab initio harmonic force field of the isolated molecule at the HF/6-311G** level of theory.[29] It is clearly seen that the experimental values do not reflect the molecular symmetry expected for the isolated molecule; that is, for the chemically equivalent bonds and links the Δ components are considerably different. In addition, the values from refinement m1 are significantly larger than the theoretical ones. To reduce this bias, a new refinement m2 was started with the calculated ADPs corresponding to the internal vibrational modes (U_{int}). In subsequent refinement cycles the shifts in the ADPs were restricted, via rigid-link type constraints,[30] to fulfill the rigid-body motion requirement.[31] This was achieved by invoking 148 independent rigid-link constraints, which meant that the MSD amplitudes along interatomic links were kept equal ($\Delta_{ik}0$) for the necessary number of atom pairs. This procedure is equivalent to the fit of the **T**, **L**, and **S** tensors of the rigid-body motion model,[32] and thus it allows preserving the characteristics of the internal vibrational modes calculated by means of the normal coordinate analysis of the isolated molecule. The statistical figures of merit of the two refinements are compared in Table 1. The constrained refinement m2, with a much higher reflections-to-variables ratio, is evidently superior to that of m1. The multipole parameters based on model m2 are deposited.

Quantum Chemical Calculations

The experimental charge density determination was completed with ab initio calculations to derive theoretical densities. All calculations were performed with the GAUSSIAN92 program package[29] at the Hartree−Fock (HF) level of theory. An optimization was carried out with the 6-311G** basis set starting from the X-ray structural data at 15 K; however the molecular C_s symmetry was imposed as a constraint. As convergence criterion the threshold limits of 0.00045 and 0.0018 au were applied for the maximum force and displacement, respectively. A summary of experimentally and theoretically obtained bond distances is given in Table 5. Based on the model obtained from the above-described optimization, an approach toward the transition state **11c** was calculated at the HF/6-31G** level by a stepwise lengthening of the distance C2−C8. The transition state **11c** was reached at an energy difference to the ground state of 7.75 kcal/mol, and the full optimization of the C_{2v} symmetric model **11c** yielded C(2)−C(6)═C(4)−C(8) = 2.015 Å, compared to the room-temperature X-ray structure, where this distance was 1.966(3) Å.

It is well-known that the Hartree−Fock level of theory does not adequately represent systems undergoing the Cope rearrangement.[33] In particular, electron correlation must be included to obtain accurate relative energies for the C_{2v} structures of semibullvalenes.[1,2] Our AM1results on the bisanhydride **11** clearly indicate that the homoaromatic species **11c** (in the gas phase) is the ground state.[1e] Similarly our preliminary results using correlated ab initio and density functional theory methods also show **11c** to be the ground state.[34]

Results and Discussion

The major result of the ultralow-temperature structure analyses in the range 123−15 K is that the most significant change in the molecular geometry of **11** from the time-averaged symmetric form to the lower symmetric C_s form **11a** or **b** had already taken place in the higher temperature range between room temperature and 123 K. In the temperature range considered in this study there is only a marginal change in the C(2,8) and C(4,6) distances by less than 0.04 and 0.03 Å, respectively; see Table 6 or Figure 2.

Nevertheless, it was important to check, at the stage of the conventional refinement, for a possible disorder structure which would manifest itself also in the mean-square displacement (MSD) tensor components. To reveal such an effect, the atomic anisotropic displacement parameters (ADPs) obtained from the structure refinement against the 15 K data are to be examined. A

(29) Frisch, M. J.; Trucks, G. W.; Schlegel, H. B.; Gill, P. M. W.; Johnson, B. G.; Wong, M. W.; Foresman, J. B.; Robb, M. A.; Head-Gordon, M.; Replogle, E. S.; Gomperts, R.; Andres, J. L.; Raghavachari, K.; Binkley, J. S.; Gonzalez, C.; Martin, R. L.; Fox, D. J.; Defrees, D. J.; Baker, J.; Stewart, J. P.; Pople, J. A. *Gaussian, 92/DFT*, Revision G.1; Gaussian Inc.: Pittsburgh, PA, 1993.

(30) Didisheim, J.-J.; Schwarzenbach, D. *Acta Crystallogr.* **1987**, *A43*, 226.

(31) Schomaker, V.; Trueblood, K. N. *Acta Crystallogr.* **1968**, *B24*, 63.

(32) Koritsanszky, T. *Acta Crystallogr.*, in preparation.

(33) Borden, W. T.; Davidson, E. R. *Acc. Chem. Res.* **1996**, *29*, 67.

(34) Williams, R. V.; Tolbert, R. W.; Edwards, W. D. Unpublished results.

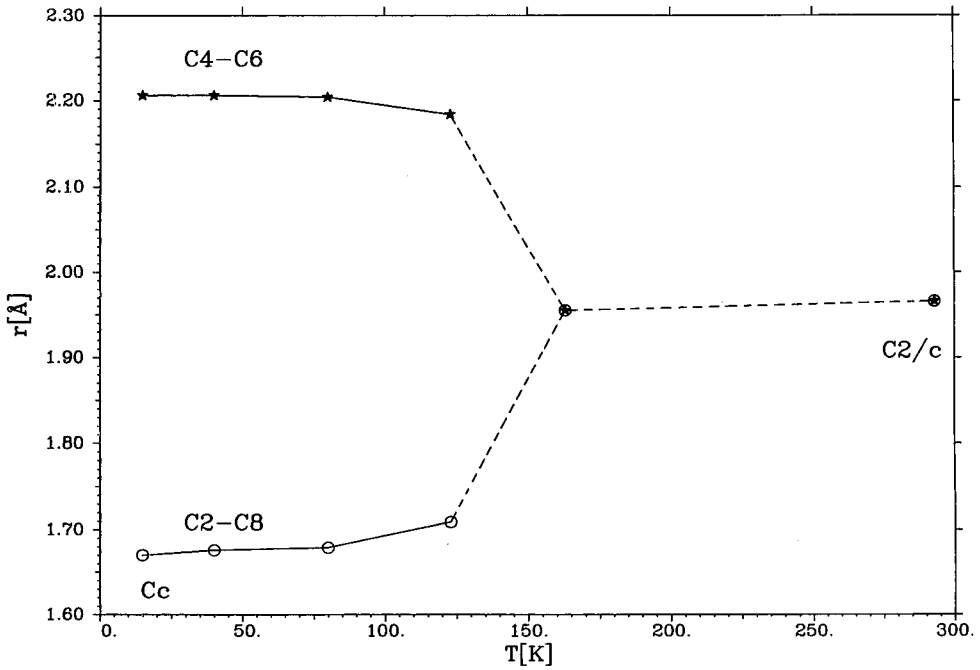

Figure 2. Distances C(4)−C(6) and C(2)−C(8) for **11** in the temperature range 295−15 K.

Table 6. C(2,8) and C(4,6) Distances for 11

temperature (K)	*C*(2,8) (Å)	*C*(4,6) (Å)	$\sum_r{}^d$ (Å)	K^d
293	1.966(3)[1d]	1.966(3)[1d]	3.932	1.000[b]
243	1.963(3)[a]	1.963(3)[a]	3.926	1.000[b]
163	1.955(2)[a]	1.955(2)[a]	3.910	1.000[b]
148	1.726(6)[a]	2.160(6)[a]	3.886	0.117
123	1.679(4)[1d]	2.197(4)[1d]	3.876	0.017
	1.709(4)[c]	2.184(4)[c]	3.893	0.079
80	1.679(2)[c]	2.204(2)[c]	3.883	0.017
40	1.676(2)[c]	2.206(2)[c]	3.882	0.011
15	1.670(1)[c]	2.206(1)[c]	3.876	

[a] Unpublished results kindly provided by Professor Dick van der Helm. See also ref 1d. [b] The apparent symmetry results from equal populations of **11a** and **11b**. [c] This work. [d] $\sum_r$ is defined as the sum of the C(2,8) and C(4,6) distances; for definition of *K* see formula 1.

plausible approach is to analyze them in terms of the rigid-body motion model.[31] To reveal outliers, i.e., anomalous tensor components, the ADPs of the C(2)/C(8) and C(4)/C(6) atom pairs were excluded from the fit. The ADPs predicted by the rigid-body motion model (calculated from the **T**, **L**, and **S** tensors) were then subtracted from those observed, and the residuals $\Delta U = U(\text{exp}) - U(\text{TLS})$ were visualized with the use of the computer graphics program PEANUT[35] in terms of residual root-mean-square displacement (RMSD) surfaces at each atomic site. In Figure 3a the solid/dotted lobes display directions along which the rigid-body model under-/overestimates the atomic displacements with respect to the observed ADPs. Since the RMSD surfaces of the four atoms in question are comparable in size to those of the other atoms and no directional correlation can be recognized in their mutual orientation, we concluded that disorder plays no recognizable role in the 15 K structure.

The differences in the ADPs obtained by the two multipole refinement models (see section on multipole refinement) can similarly be vizualised. In Figure 3b the RMSD surfaces represent residual MSD tensors calculated by subtracting the equivalent tensor components given by model m2 from those of m1. The residuals are significant and they are especially pronounced for the oxygen atoms and the carbon atoms of the methyl group. This bias in the ADPs of model m1 is accompanied by a bias in the multipole populations. There are significant differences, especially in the quadrupole populations ($l = 2$), between the two sets of parameters estimated via the two refinement models. The corresponding static electron densities differ considerably in the near vicinity of the nuclei but only slightly in the bonding regions.

As qualitative results, some deformation density contour maps are shown in the two planar fragments defined on one side by the carbon atoms C(2), C(8), C(9), C(10) (plane I) and on the other side by C(4), C(6), C(13), C(14) (plane II) (Figure 4). Figure 4a shows a simple X−X map (high/low-order cutoff at $\sin\theta/\lambda = 0.8$ Å^{-1}) to compare with the corresponding theoretical map from the ground-state optimization (Figure 4b).

Both methods give a rather weak but clearly visible deformation density maximum in the C(2)−C(8) bond, but no density accumulation is observed between the C(4) and C(6) atoms.

At a calculated bond distance of 1.8 Å the C(2)−C(8) bond peak is reduced (Figure 4c) in comparison to that found at the experimental geometry. At the transition state this deformation density has almost completely disappeared; only a very low-density region indicated by a contour line of 0.005 e/Å^3 is left (see Figure 4d). For the 15 K experimental structure and the theoretical model obtained from the ground-state ab initio optimization a full topological analysis following Bader's approach was made.[36] The topological analysis of the theoretical densities was performed with the program PROAIM,[37] while the experimental $\rho(r)$ was analyzed with the property program XDPROP of the system XD.[24] In both

(35) Hummel, W.; Hauser, J.; Bürgi, H.-B. *J. Mol. Graphics* **1990**, *8*, 214.

(36) Bader, R. F. W.: *Atoms in Molecules−a Quantum Theory*; Clarendon Press: Oxford, 1990.

(37) Cheeseman, J.; Keith, T. A.; Bader, R. F. W. *AIMPAC progam package*; McMaster University: Hamilton, Ontario, 1992.

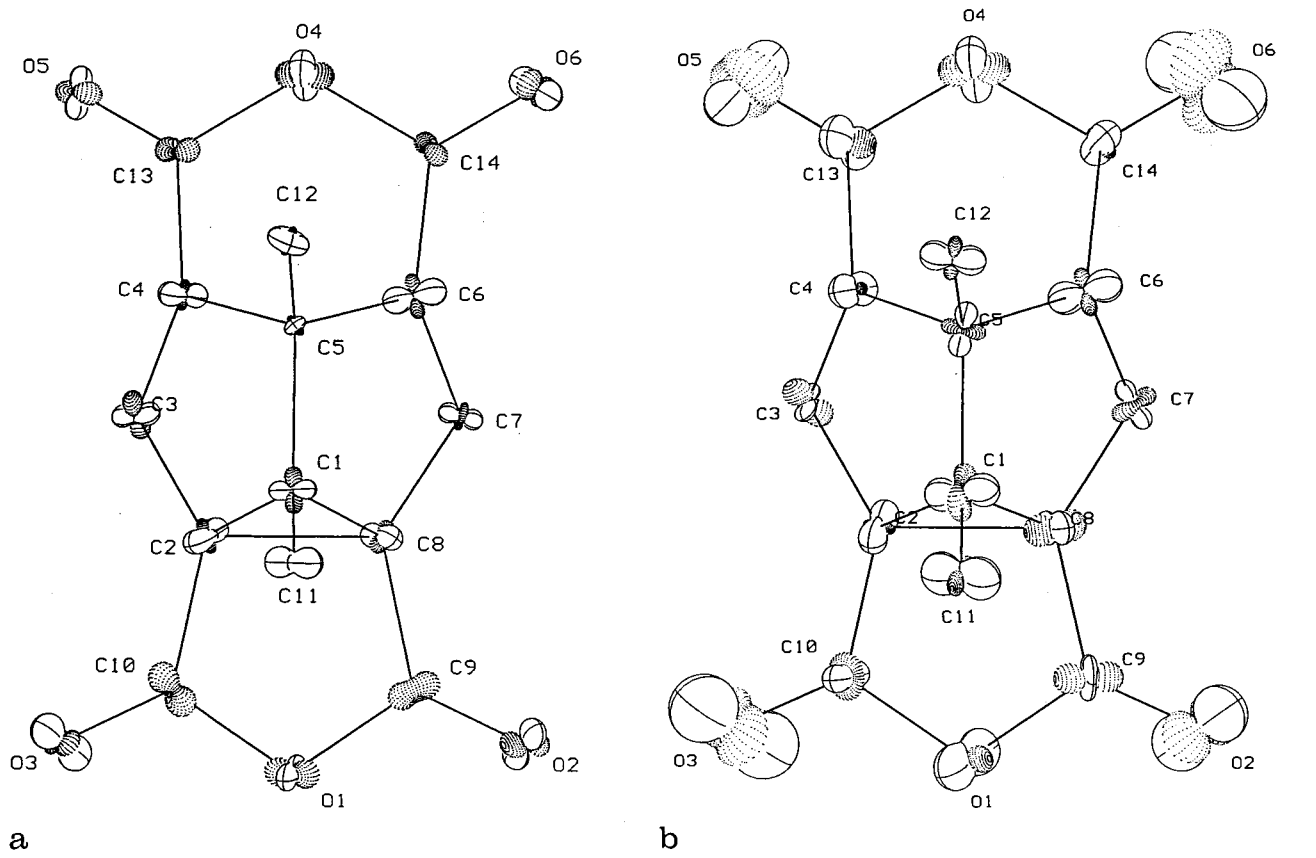

Figure 3. (a) "Peanut" representation with respect to $\Delta U_{ij} = U_{ij}(\text{exp}) - U_{ij}(\text{TLS})$; see also text. (b) Corresponding representation with $\Delta U_{ij} = U_{ij}(\text{model m1}) - U_{ij}(\text{model m2})$.

cases the Laplacian distributions were evaluated, and all bond critical points (CPs) and valence shell charge concentrations (VSCC, the (3,+3) CPs of $\nabla^2\rho(r)$) were located.

Figure 5 compares the negative Laplacian functions, in the planes of the three-membered rings C(1), C(2), C(8) (plane III) and C(4), C(5), C(6) (plane IV), calculated from the wave function at the HF/6-311G** level and from the experimental static $\rho(r)$. The topological equivalence of the functions obtained by the two methods is evident in both the bonding and nonbonding areas. In the bond C(2)−C(8) the charge concentration forms a continuous region between the atoms, which is a characteristic feature of covalent interaction that is not seen at C(4)−C(6). A quantitative comparison of the results can be given in terms of bond topological properties, such as the value of $\rho(r_b)$ and its Laplacian ($\nabla^2\rho(r_b)$ at the bond critical point (CP, located at r_b where $\nabla\rho(r_b) = 0$). In terms of these values, listed in Table 7, the atomic interactions can be characterized. A relatively high value of $\rho(r_b)$ where $\nabla\rho(r_b) = 0$ is a sign for covalent (*shared*) interaction. An important observation is that no bond CP was found between the C(4) and C(6) atoms. There is an excellent agreement between the theoretical and experimental values of $\rho(r_b)$, but the same is not true for the $\nabla^2\rho(r_b)$ values. This is likely due to the pure quality basis set applied, which is not extended enough to give a satisfactory representation of the Laplacian distribution in polar bonds. It has been shown[38] that diffuse functions are needed to describe the valence shell charge concentrations of the oxygen atom of the C=O polar bond. The C(2,8) and C(4,6) distances for **11** at various temperatures are shown in Table 6 and graphically in Figure 2. True to Quast's hypothesis,[14] the sum of these distances ($\sum_r$) is relatively constant. In semibullvalenes with a very low barrier to the Cope rearrangement $\sum_r$ is considerably larger (3.97−3.99 Å) than the corresponding sum (3.85−3.93 Å) in the less fluxional semibullvalenes.[14] Although **11** is highly fluxional, its $\sum_r$ is in the range of the more slowly rearranging Cope systems. This anomaly is not too surprising, as the bisannelation obviously causes some compression of the C(2,8) and particularly the C(4,6) distances compared with the corresponding distances in the "open" (not annelated) semibullvalenes. We used the relationship (1), developed by Quast,[14] to estimate the equilibrium constant (K) for the Cope equilibrium between the nondegenerate tautomers **11a** and **11b** (Table 6):

$$K = \frac{C(2,8)_{av} - C(2,8)}{C(4,6) - C(2,8)_{av}} \qquad (1)$$

$C(2,8)_{av}$ = observed average C(2,8) distance

$C(2,8)$ = limiting value for the C(2,8) distance (assumed to be that at 15 K)

$C(4,6)$ = limiting value for the C(4,6) distance (assumed to be that at 15 K)

The equilibrium constant over the temperature range 293−163 K, where the structures show apparent C_2

(38) Flaig, R.; Koritsanszky, T.; Zobel, D.; Luger, P *J. Am. Chem. Soc.* **1998**, *120*, 2227.

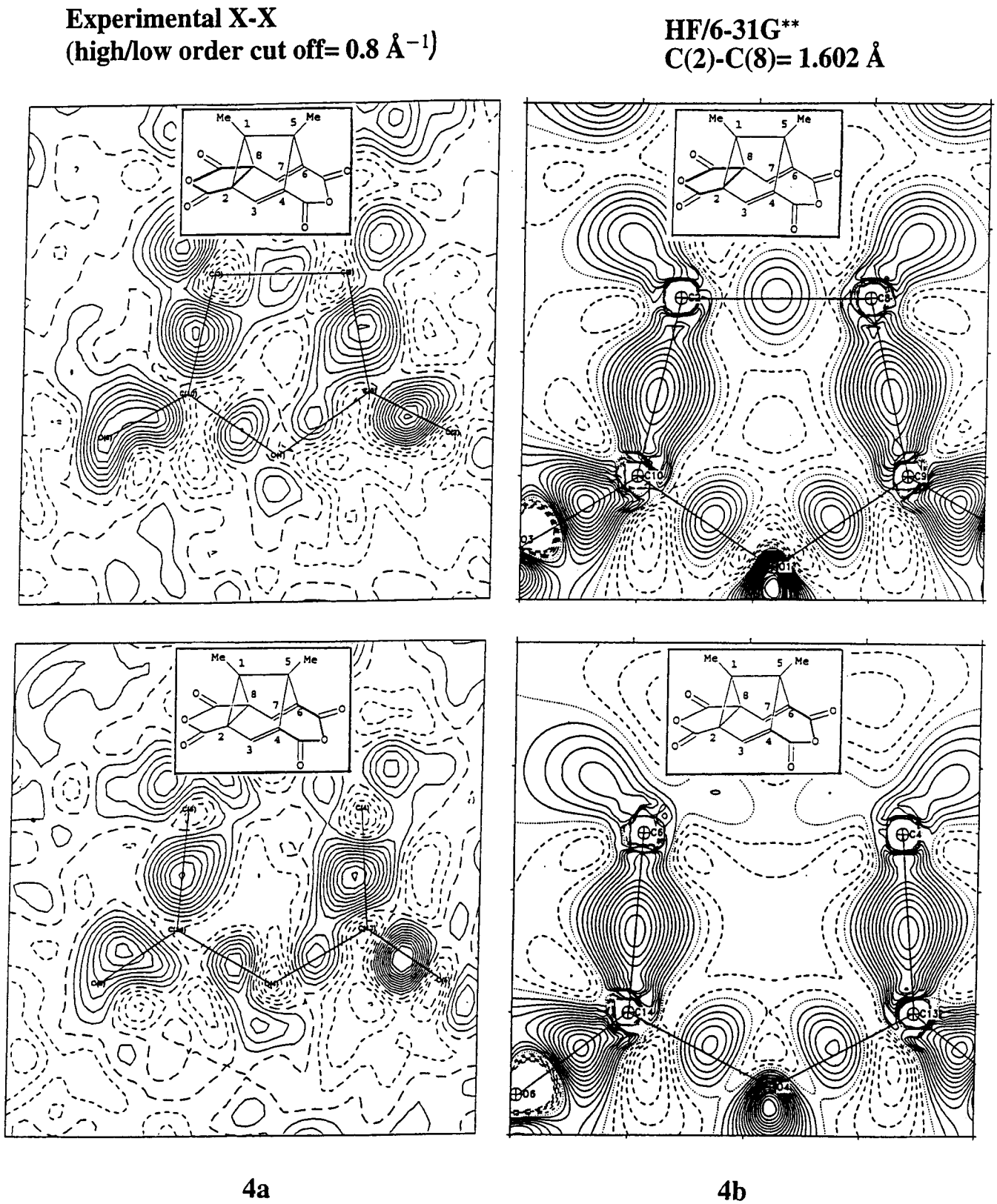

Figure 4. Deformation densities in plane I (above) and plane II (below) of **11**. (a) Experimental X−X at 15 K. (b) Theoretical density from HF/6-31G** optimization with C(2)−C(8) kept at 1.602 Å.

symmetry, is assumed to be 1. Furthermore, it is assumed that at temperatures below 40 K the equilibration is frozen out. From a plot of ln K against $1/T$ (Figure 6) there is a reasonably linear relationship in the temperature range 148−80 K, from which the difference in free energy between **11a** and **11b** was assessed to be $\Delta G°$ = 0.162 kcal/mol. The errors in this procedure are significant, and the estimated value of $\Delta G°$ should only be considered as an indicator of the order of magnitude of this quantity. The inequivalence of **11a** and **11b** is, of course, purely a solid-state effect.

Our X-ray and solution-phase NMR data reveal that

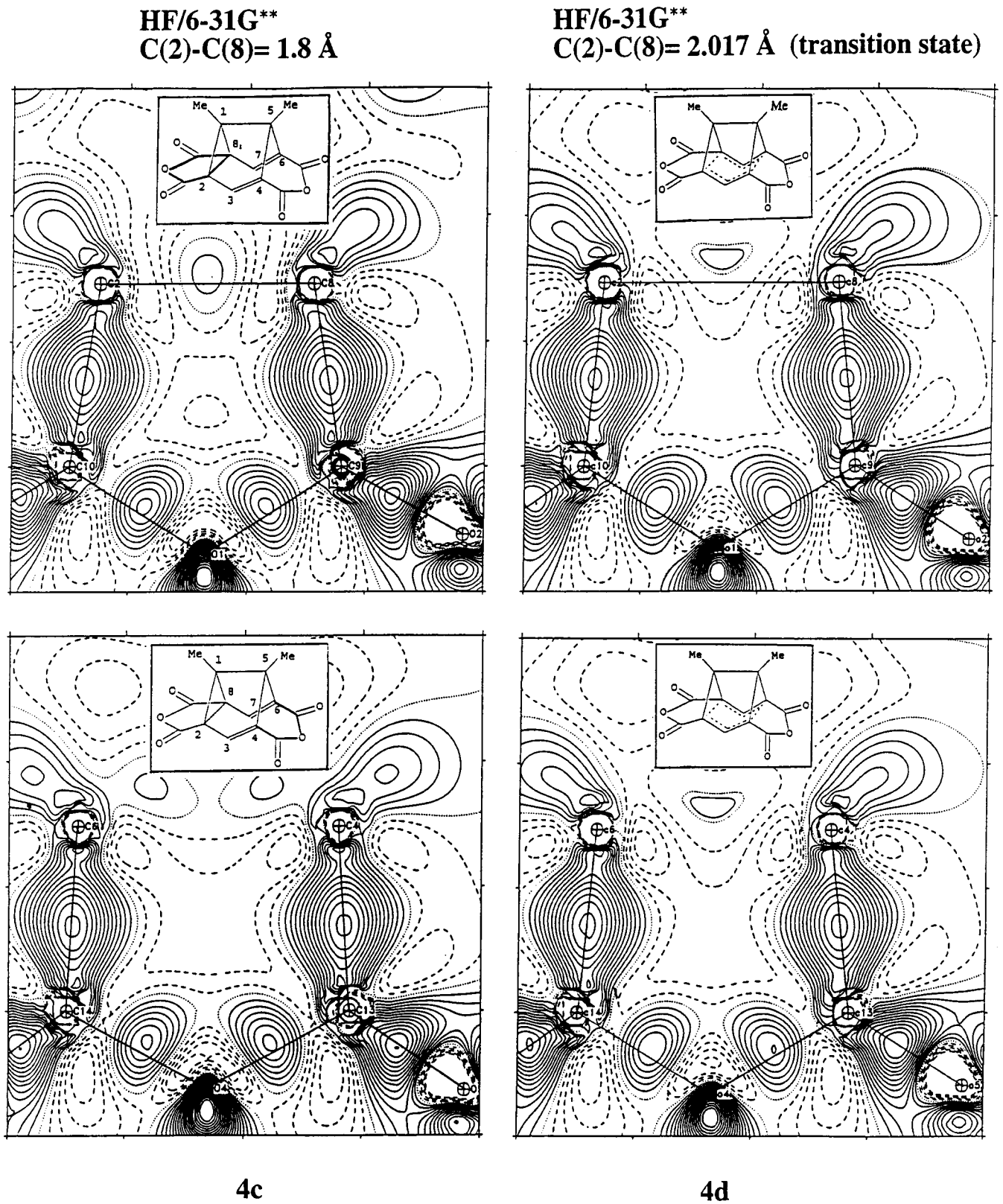

(*Figure 4 caption, continued*) (c) Same as b, but C(2)−C(8) fixed at 1.8 Å. (d) Same as b, but C(2)−C(8) = 2.017 Å, corresponding to the transition state **11c**. Contour lines are drawn at increments of 0.05 e/Å^3, zero line dotted. Exception: In part d the solid line between C(4) and C(6) represents a 0.005 e/Å^3 region.

11 is a localized Cope system with an extremely low barrier to the Cope rearrangement (less than 3.3 kcal/mol in the solution phase).[1d,e] However our correlated semiempirical, ab initio, and DFT calculations (all of proven reliability) clearly indicate a homoaromatic ground state (**11c**) for **11**.[1d,e,34] The calculations, of course, only strictly apply to the gas phase. It is recognized that in the condensed phases matrix fields may radically change the geometry of a molecule compared with its gas-phase structure.[39] The asymmetric crystalline environment for

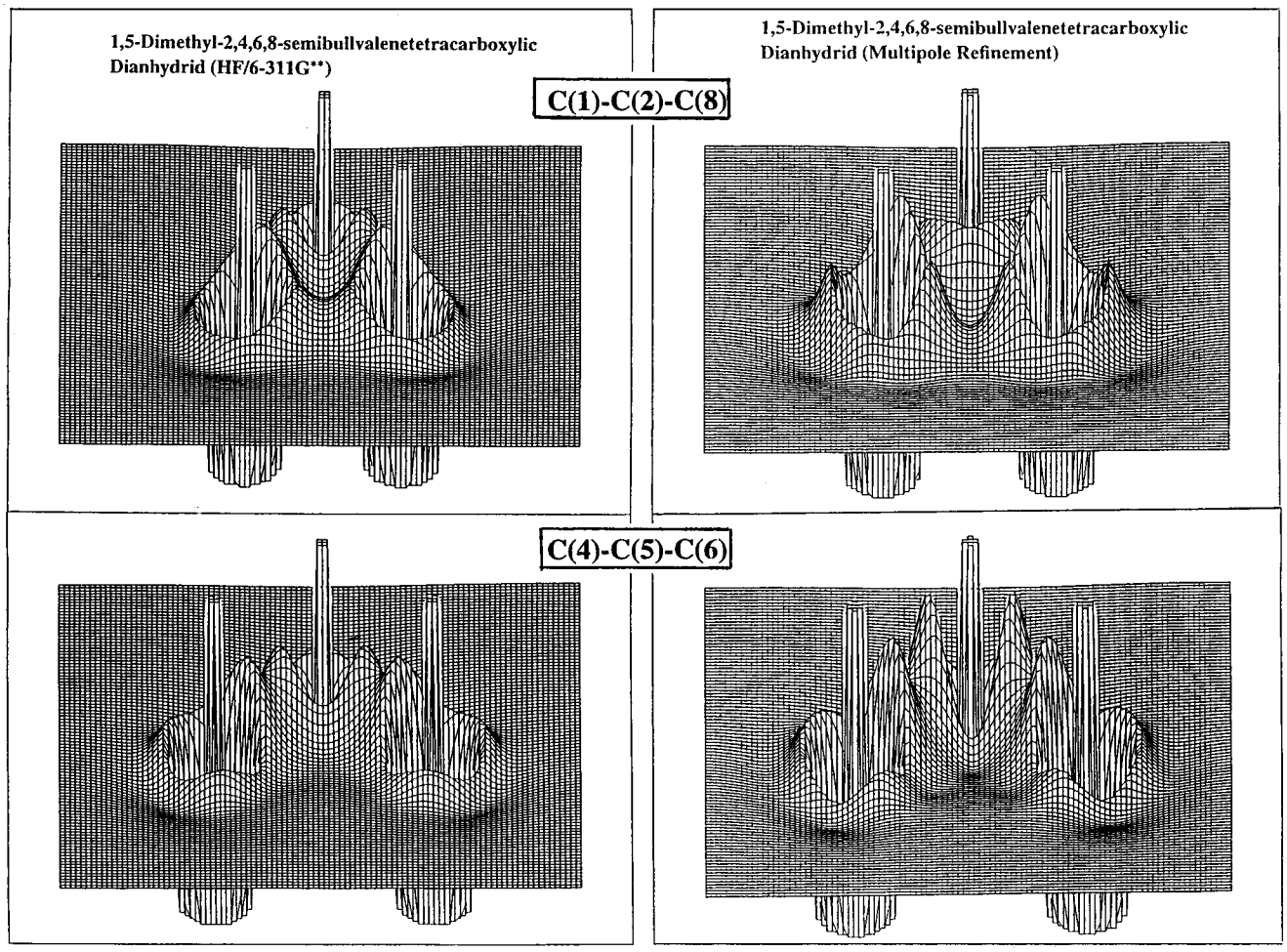

Figure 5. Negative Laplacian distributions in plane III (C(1)−C(2)−C(8)) (above) and plane IV (C(4)−C(5)−C(6)) (below) from theoretical calculation at the HF/6-311G** level and from the static $\rho(\vec{r})$ at 15 K.

Table 7. Topological Parameters of Bonds Formed by Non Hydrogen Atoms[a]

	HF/6-311G**		experimental model m2	
bond	$\rho(r_b)$	$\nabla^2\rho(r_b)$	$\rho(r_b)$	$\nabla^2\rho(r_b)$
C(2)−C(8)	1.36	−5.64	1.38(3)	−1.0(1)
C(2)−C(1)	1.71	−13.75	1.67(4)	−7.7(1)
C(1)−C(5)	1.69	−15.50	1.57(4)	−8.3(1)
C(4)−C(5)	1.74	−16.42	1.84(4)	−16.0(2)
C(4)−C(6)				
C(2)−C(10)	1.91	−20.30	2.08(4)	−15.0(2)
C(2)−C(3)	1.89	−19.28	1.94(5)	−18.0(2)
C(4)−C(13)	1.92	−20.76	1.63(5)	−10.8(2)
C(3)−C(4)	2.39	−27.70	2.24(5)	−20.1(2)
C(1)−C(11)	1.75	−17.05	1.74(5)	−14.5(1)
C(5)−C(12)	1.73	−16.61	1.69(5)	−14.5(1)
C(10)−O(1)	1.95	−4.66	1.98(4)	−14.2(2)
C(10)−O(3)	3.08	7.68	3.02(5)	−28.2(3)
C(13)−O(4)	1.87	−4.45	1.96(4)	−13.8(2)
C(13)−O(5)	3.08	7.55	3.01(5)	−28.0(3)

[a] $\rho(r_b)$ in e/Å^3, $\nabla^2\rho(r_b)$ in e/Å^5.

each molecule of **11** in its thermodynamically preferred *Cc* space group, which contains four molecules with a glide plane relation between molecular pairs, will certainly favor the localized C_s form over the delocalized C_{2v} **11c**. No doubt, packing forces sufficiently perturb the potential energy surface of **11** to result in a localized Cope ground state. However, they cannot be quantified from

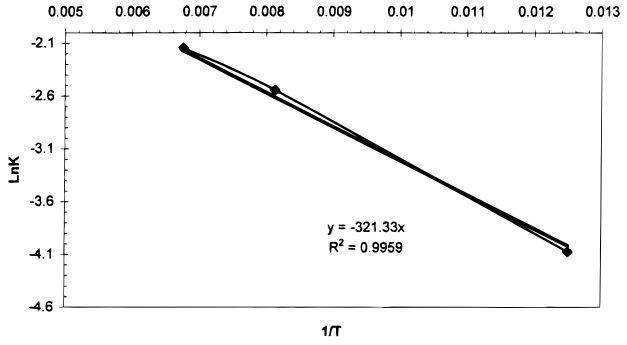

Figure 6. Plot of ln *K* against 1/*T*.

the X-ray data as there are not short contacts indicating close intermolecular interactions. The shortest non hydrogen contacts are for O···O, which are all between 3.2 and 3.3 Å and hence beyond the van der Waals distance for oxygen (3.04 Å).[40] The uncorrelated levels of theory tend to underestimate the stability of the delocalized homoaromatic forms of the semibullvalenes,[1,2a] serendipitously resulting in a HF localized ground state for **11** in agreement with the low-temperature X-ray structures. We are currently investigating some properties of **11** in the gas phase.

(39) For example, see: Wiberg, K. B.; Keith, T. A.; Frisch, M. J.; Murcko, M. *J. Phys. Chem.* **1995**, *99*, 9072, and references therein.

(40) Bondi, A. *J. Phys. Chem.* **1964**, *68*, 441.

(41) Johnson, C. K. **1976**. *ORTEP II*; Report ORNL-5138; Oak Ridge National Laboratory: TN.

Conclusion

Correlated ab initio (MP2) and density functional theory (DFT) methods[34] as well as semiempirical calculations[1d,e] predict a symmetrical homoaromatic ground state for the dianhydride **11**. However, at the Hartree–Fock (HF) level of theory the localized geometry (**11a** or **11b**) is preferred. This HF geometry is in remarkable agreement with the experimental structure determined at 15 K. The experimental and HF electron densities for **11** are also in excellent accord. Consideration of the experimental electron density plots (Figures 4a and 5) clearly reveals a "normal cyclopropyl σ-bond" between C(2,8) and very sparse density between C(4,6), corresponding to little or no interaction between these latter two centers. These results certainly confirm that in the solid state **11** is not homoaromatic. The experimental data at 15 K provides limiting values of structural parameters for a single tautomer of **11**. In particular, the C(2,8) and C(4,6) distances and $\sum_r$ are extremely useful base values for a bisannelated semibullvalene with an exceptionally low activation barrier to the Cope rearrangement.[1d,e] Comparison of these base values with the corresponding values obtained for other bisannelated semibullvalenes, currently the target of syntheses, will facilitate the characterization of these fascinating molecules.

Acknowledgment. Part of this work was funded by the Deutsche Forschungsgemeinschaft (DFG, Az LU 222/20-1), Bonn, Germany, and by the Fonds der Chemischen Industrie, Frankfurt, Germany.

Supporting Information Available: Tables of crystal data and structure refinement, atomic coordinates, bond lengths and angles, anisotropic displacement parameters, hydrogen coordinates, isotropic displacement parameters, and multipole population parameters. This material is available free of charge via the Internet at http://pubs.acs.org.

JO981703Q